THE JOURNAL OF BIOLOGICAL CHEMISTRY VOL. 289, NO. 24, pp. 17100–17110, June 13, 2014

The UvrD303 Hyper-helicase Exhibits Increased Processivity*

Received for publication, March 13, 2014, and in revised form, April 30, 2014 Published, JBC Papers in Press, May 5, 2014, DOI 10.1074/jbc.M114.565309

Matthew J. Meiners[‡], Kambiz Tahmaseb[‡], and Steven W. Matson[‡§1]

From the [‡]Department of Biology, [§]Curriculum in Genetics and Molecular Biology, University of North Carolina at Chapel Hill, Chapel Hill, North Carolina 27599

Background: A mutation within the 2B subdomain of UvrD increases helicase activity and impacts phenotype.
Results: The unwinding processivity is increased in the UvrD303 mutant.
Conclusion: The 2B subdomain of UvrD plays an integral role in regulating helicase activity.
Significance: Intramolecular interactions mediate proper activity for UvrD in DNA repair processes.

DNA helicases use energy derived from nucleoside 5′-triphosphate hydrolysis to catalyze the separation of double-stranded DNA into single-stranded intermediates for replication, recombination, and repair. *Escherichia coli* helicase II (UvrD) functions in methyl-directed mismatch repair, nucleotide excision repair, and homologous recombination. A previously discovered 2-amino acid substitution of residues 403 and 404 (both Asp → Ala) in the 2B subdomain of UvrD (*uvrD303*) confers an antimutator and UV-sensitive phenotype on cells expressing this allele. The purified protein exhibits a "hyper-helicase" unwinding activity *in vitro*. Using rapid quench, pre-steady state kinetic experiments we show the increased helicase activity of UvrD303 is due to an increase in the processivity of the unwinding reaction. We suggest that this mutation in the 2B subdomain results in a weakened interaction with the 1B subdomain, allowing the helicase to adopt a more open conformation. This is consistent with the idea that the 2B subdomain may have an autoregulatory role. The UvrD303 mutation may enable the helicase to unwind DNA via a "strand displacement" mechanism, which is similar to the mechanism used to processively translocate along single-stranded DNA, and the increased unwinding processivity may contribute directly to the antimutator phenotype.

DNA helicases are ubiquitous motor proteins that transiently convert duplex DNA into single-stranded DNA (ssDNA)[2] using energy derived from nucleoside 5′-triphosphate (NTP) hydrolysis for a wide variety of biological processes including DNA replication, repair, and recombination (1–5). Thus, helicases are vital for the maintenance of the genome and mutations within helicase-encoding genes in humans have been linked to both cancer and aging disorders (6–8).

In *Escherichia coli*, the product of the *uvrD* gene, DNA helicase II (UvrD), has been shown to function in two fundamental DNA repair processes: nucleotide excision repair (NER) (9) and methyl-directed mismatch repair (MMR) (10, 11). In NER, UvrD acts in conjunction with the UvrABC excision nuclease and DNA polymerase I to remove short 12–13-base oligonucleotides containing a wide variety of bulky lesions including pyrimidine dimers (9). UvrD also participates in the MMR pathway by initiating unwinding at the nicked d(GATC) site created by MutH and displacing the nascent error-containing strand of DNA, which is degraded by exonucleases and subsequently resynthesized by DNA polymerase III (10, 12). UvrD has been suggested to have a role in other cellular processes, such as displacement of the RecA protein from ssDNA during conjugative recombination (13). However, this role for UvrD is not as well understood. The *uvrD* gene encodes a 720-amino acid, 82-kDa Superfamily 1A (SF1A) helicase with well characterized 3′ to 5′ unwinding and translocase directionality. Consistent with other SF1 helicases, UvrD contains seven conserved motifs and two structural domains (1 and 2) each with two subdomains (A and B) (14–21).

Crystal structures for both UvrD (14, 22) and the structurally related (38% amino acid identity) Rep helicase (20) have been reported (see Fig. 1 for UvrD). Each protein is capable of adopting two conformations, open and closed, with the major difference between the two conformations being the orientation of the 2B subdomain. In the "open" form the 2B subdomain is stacked above the 2A subdomain and no contacts are made between the 2B and 1B subdomains. To adopt the alternate "closed" structure, the 2B subdomain rotates about a flexible hinge connected to the 2A subdomain and "closes" onto the 1B subdomain. The magnitude of the 2B subdomain rotation as the helicases modulate between the open and closed conformations has been reported to be 130° in Rep and 160° in UvrD. Although it is known that these SF1 helicases can adopt these alternate conformations, it is not clear why there are two alternate conformations. The related SF2 helicases (*e.g.* the hepatitis NS3 helicase) lack the equivalent of the 2B subdomain (23, 24). Consequently, the role of the 2B subdomain in SF1 helicases is not well understood.

Previous studies (25, 26) have examined what role, if any, the 2B subdomain of Rep plays in the activity of this protein. It was concluded that the 2B subdomain is most likely a regulatory domain because deletion of this subdomain stimulates the unwinding and translocase activity of the protein in addition to activating the helicase activity of a RepΔ2B monomer. How-

* This work was supported, in whole or in part, by National Institutes of Health Grant GM33476.
[1] To whom correspondence should be addressed: CB 3280, Coker Hall, University of North Carolina, Chapel Hill, NC 27599-3280. Tel.: 919-962-0005; Fax: 919-962-1625; E-mail: smatson@bio.unc.edu.
[2] The abbreviations used are: ssDNA, single-stranded DNA; NER, nucleotide excision repair; MMR, methyl-directed mismatch repair; UvrD, DNA helicase II; ATPγS, adenosine 5′-*O*-(thiotriphosphate).

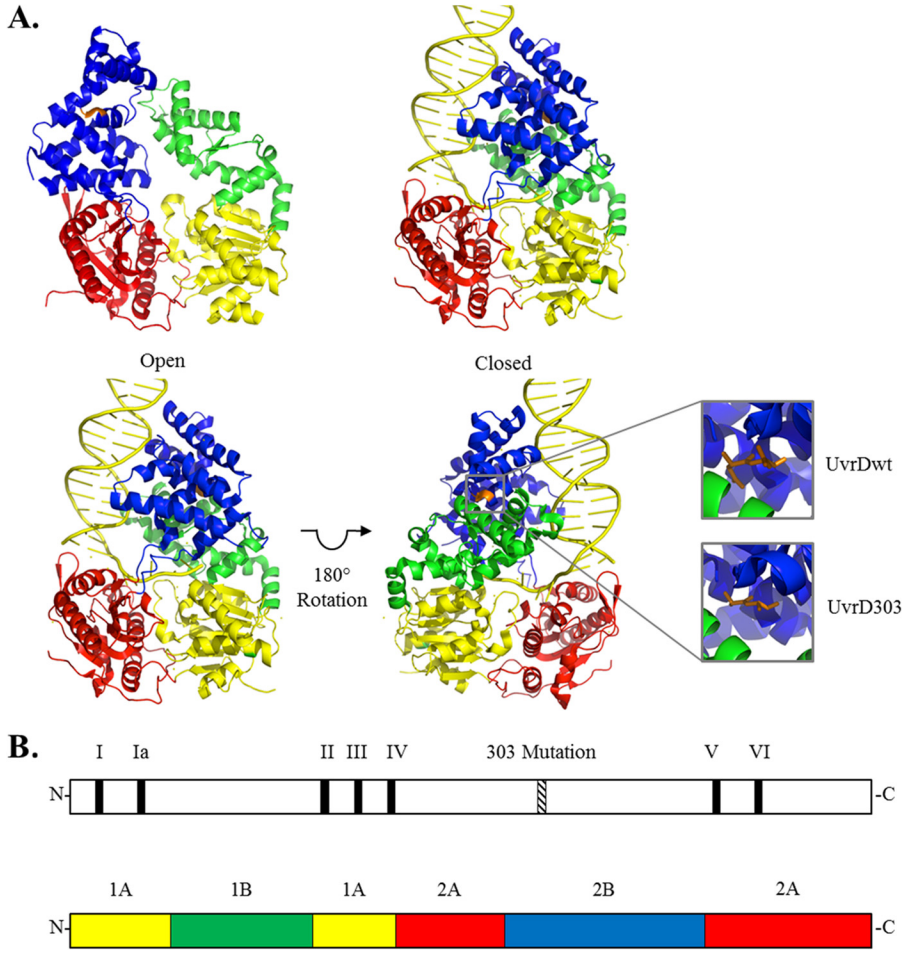

FIGURE 1. **Models of *E. coli* UvrD and the mutant UvrD303 helicase in open and closed conformations.** *A*, *upper panel*, ribbon diagram of the apo-structure of UvrD in the open conformation (Protein Data Bank code 3LFU) and ribbon diagram of UvrD bound to partial duplex DNA in the closed conformation. *Lower panel,* ribbon diagram of UvrD bound to partial duplex DNA in the closed conformation (left side) and rotated 180° (right side) (Protein Data Bank code 2IS2) (33, 14). The 1A subdomain is shown in *yellow*, the 1B subdomain is shown in *green*, the 2A subdomain is shown in *red*, the 2B subdomain is shown in *blue*. Mutated residues are denoted in *orange* and by stick representation. For amino acid substitution in UvrD303 (Asp to Ala), rotamers were selected for minimum steric hindrance. Molecular images were generated with the PyMOL Molecular Graphics System, version 1.3, Schrödinger, LLC. *B*, *top panel,* a schematic representation of the seven conserved helicase motifs (15) of UvrD. The *hashed box* represents the placement of the 303 mutation. *Bottom panel,* a schematic representation of the four structural subdomains of UvrD. The two graphics are aligned such that the placement of the 303 mutation within the 2B subdomain can be seen.

ever, the role of the 2B subdomain in UvrD continues to be debated (14). The two prevailing hypotheses suggest that either the 2B subdomain is required to make direct double-stranded DNA interactions, which allow the helicase to bind various substrates, or that the 2B subdomain functions in a regulatory role, modulating helicase activity. Direct studies of a corresponding deletion of the 2B subdomain in UvrD have not been reported due to the apparent lethality of the expression of UvrDΔ2B (25).

Previous work by Zhang *et al.* (27) isolated an allele of *uvrD* that contained two point mutations within the 2B subdomain. In this mutant form of UvrD, named UvrD303, the native amino acids at positions 403 and 404 (both aspartic acids) were mutated to alanines (Fig. 1). When UvrD303 was expressed in place of the wild-type protein, from either the chromosome or a high copy number plasmid, cells exhibited antimutator, UV-sensitive and hypo-recombinant phenotypes (27, 28). When purified and analyzed *in vitro*, UvrD303 exhibited a 10-fold increase in unwinding activity compared with its wild-type counterpart. This increased activity led to UvrD303 being referred to as a "hyper-helicase." Interestingly, neither D403A nor D404A alone were sufficient to convey this hyper-helicase activity (27).

This article presents a biochemical characterization of the UvrD303 mutant including a possible explanation for how the 2B subdomain mutation increases the unwinding activity of the helicase. Using single turnover rapid quench helicase assays, we have shown that the processivity of UvrD303, as a DNA helicase, is ~10-fold higher than that of wild-type UvrD. We speculate that the mutation alters the ability of the 2B subdomain to properly adopt a closed conformation, as referred to above. The closed conformation appears to be important for normal endogenous helicase activity of wild-type UvrD as evidenced by the phenotype of cells expressing UvrD303.

MATERIALS AND METHODS

Helicase Purification—The *uvrD* gene was amplified via polymerase chain reaction from genomic K12 λ^+ F^+ DNA using the following primers: forward primer, 5′-CGGCGGTGCCATGGACG-3′ and reverse primer, 5′-TACCGACTCCAGCCGGGC-3′. The 5′ terminus of the reverse primer was

phosphorylated with T4 polynucleotide kinase to facilitate blunt end ligation. The pTYB4-His vector was digested using the restriction enzymes NcoI and SmaI (New England Biolabs) and the resulting 7.5-kb DNA fragment was purified via agarose gel electrophoresis and excision of the DNA followed by use of a Qiagen quick spin purification column. The purified digested vector was treated with shrimp alkaline phosphatase to reduce the likelihood of vector re-ligation in subsequent cloning reactions. The *uvrD* containing PCR product was digested with the restriction enzyme NcoI and purified in a manner similar to the vector. The resultant digested vector and PCR insert were ligated using T4 ligase. Using this cloning technique, the SmaI site in pTYB4-His is destroyed, but will ensure that only a C-terminal glycine will be added to the protein after purification, yielding essentially native protein. This construct enabled the rapid purification of the helicase as previously described (29). The *uvrD303* allele was constructed using site-directed mutagenesis. A QuikChange PCR was performed using primers of the following sequence: forward, 5′-CTGATTGCCAACCGCAACGACGACGCGGCCTTTGAGCGTGTG-3′ and reverse, 5′-CACACGCTCAAAGGCCGCGTCGTCGTTGCGGTTGGCAATCAG-3′ to change the codons 403 and 404 from -GACGAC- to -GCGGCC-, converting both the aspartic acids to alanines. This mutagenesis also introduced a silent NotI restriction site that was used to screen potential clones for the *uvrD303* allele. The resulting plasmid was sequenced to ensure no additional mutations had been introduced.

The construct, pTYB4-UvrD303-His, was transformed into *E. coli* strain BL21DE3*uvrD*::Tn5*mutL*::Tn10 and a 20-ml culture was grown overnight at 37 °C in ZY media (30). The overnight culture was introduced to 1 liters of ZYM5052 autoinduction media (30) and grown at 16 °C for 48 h. The cells were harvested by centrifugation, washed once with 25 ml of STE buffer (10 mM Tris-HCl (pH 8.0), 1 mM EDTA, and 100 mM NaCl), and harvested again by centrifugation. The cells were stored at −80 °C until use. The cells were lysed and the protein was purified as previously described using a combination of Talon (Clontech) and Chitin (New England Biolabs) resins to take advantage of the two affinity tags present on the overexpressed fusion protein (29). Protein that eluted from the Chitin column was dialyzed against UvrD storage buffer (31) and stored at −20 °C. The purified protein was greater than 95% homogeneous as determined by polyacrylamide gel electrophoresis in the presence of SDS. Wild-type UvrD was purified as previously described (31).

DNA Substrates—Partial duplex substrates were prepared by radiolabeling the 5′-end of oligonucleotides obtained from Integrated DNA Technologies (Coralville, Iowa) using [γ-^{32}P]ATP and T4 polynucleotide kinase (see Table 1 for sequences). A 1.1-fold excess of an unlabeled complementary oligonucleotide was annealed to the labeled strand by heating the two strands to 95 °C for 5 min and allowing them to slow cool to 25 °C overnight. The partial duplex substrate was purified from free nucleotide using a Sephadex G50 spin column and dialyzed into TEN buffer (10 mM Tris-HCl (pH 7.5), 1 mM EDTA, 50 mM NaCl). This process was used to generate the 24/64 and 90/130 partial duplex substrates. In each case the shorter DNA strand was radioactively labeled. The longer DNA strand contains a 40-base 3′-ssDNA tail to facilitate loading of UvrD.

The 243-bp partial duplex substrate was generated from a modified version of pUC19, pUC19-TS. The pUC19-TS construct was created by digesting pUC19 DNA (New England Biolabs) with BamHI and EcoRI. The insert was created by annealing the following synthetic oligonucleotides: 5′-AATTCCTCAGCAATCCTCAGCCAGGCCTCAGCTGGCCTCAGCG-3′ and 5′-GATCCGCTGAGGCCAGCTGAGGCCTGGCTGAGGATTGCTGAGG-3′. The annealing reaction created compatible ends with the BamHI- and EcoRI-digested pUC19 vector. This elongated version of pUC19 was then used in a site-directed mutagenic PCR (with the following primers: forward, 5′-GGATCCTCAGCAGTCGACCTCAGCGCATGC-3′ and reverse, 5′-GCATGCGCTGAGGTCGACTGCTGAGGATCC-3′ to create pUC19-TS, which contains a 67-bp stretch of DNA between the EcoRI and HindIII restriction sites (5′-CCTCAGCAATCCTCAGCCAGGCCTCAGCTGGCCTCAGCGGATCCTCAGCAGTCGACCTCAGCGCATG-3′) containing multiple Nt.BbvC1 nicking sites.

To produce the 243-bp partial duplex substrate 50 pmol of plasmid DNA were digested with EcoRI and SapI to completion to produce a 297-bp DNA fragment. The enzymes were heat killed at 65 °C for 20 min and the resulting DNA was purified by gel extraction using a 1.5% (w/v) (0.75% (w/v) agarose, 0.75% (w/v) low melting agarose) agarose gel. The three-nucleotide overhang generated by the SapI digest was filled in using Klenow fragment polymerase and [α-^{32}P]dCTP, dGTP, and dTTP. The fill-in reaction was incubated at 37 °C for 30 min. The purified DNA fragment, which contains seven Nt.BbvCI nickase sites (CCTCAGC), was nicked with Nt.BbvCI followed by heating to 80 °C for 20 min to denature the on average 11 nucleotide fragments generated by the nicking reaction. The resulting DNA molecule contains a 45-base 3′-ssDNA tail preceding a 243-bp duplex region. The nicked DNA was immediately applied to Qiagen QIAquick PCR Purification spin columns for purification (1 column used per 8 pmol of DNA) and eluted in TEN buffer. The final DNA concentration was determined by scintillation counting.

DNA-dependent ATPase Assays—The standard reaction mixture (40 μl) contained 25 mM Tris-HCl (pH 7.5), 3 mM $MgCl_2$, 20 mM NaCl, 5 mM 2-mercaptoethanol, 50 μg/ml of bovine serum albumin, 10 ng/μl of M13 ssDNA, [α-^{32}P]ATP (~60 nCi/μl), and 10 nM UvrD or UvrD303 helicase. For k_{cat} determinations the ATP concentration was 400 μM. For K_m determinations the ATP concentration ranged from 50 to 500 μM. All reagents except ATP were mixed and allowed to incubate on ice for 5 min. Then ATP was added and the reaction was incubated at 37 °C for 10 min. Aliquots (5 μl) were removed every 2 min and 2 μl of 5 M formic acid was added to stop the reaction. 2.5 μl of this mixture was spotted onto a thin layer chromatography plate and developed in a 0.45 M ammonium sulfate solution. Results were visualized by PhosphorImaging (GE Healthcare).

Helicase Assays—Helicase reaction mixtures (16 μl) for steady-state experiments contained 25 mM Tris-HCl (pH 7.5), 3 mM $MgCl_2$, 20 mM NaCl, 5 mM 2-mercaptoethanol, 50 μg/ml of bovine serum albumin, 3 mM ATP, helicase concentration as

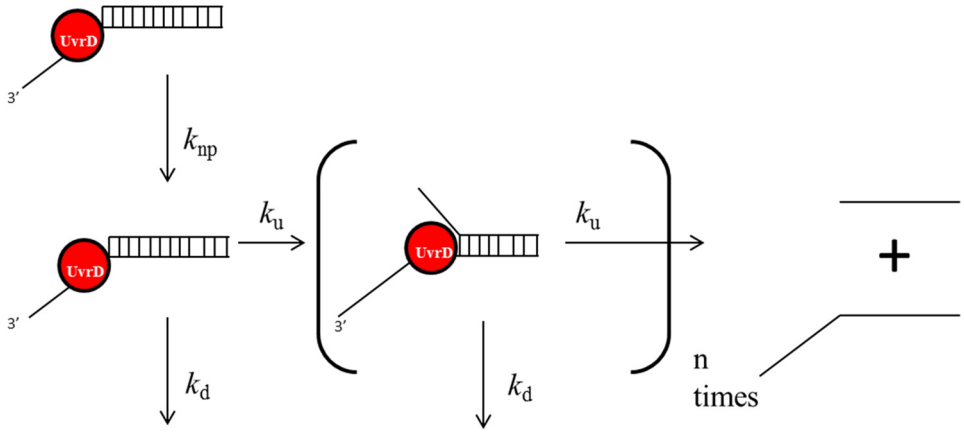

SCHEME 1. **The sequential *n*-step kinetic model.** Preformed UvrD-DNA complexes undergo a conversion to partially unwound intermediates (see inside brackets) as the pathway progresses until a fully unwound ssDNA product is generated. At each intermediate step the helicase may dissociate from the unwinding complex, k_d, or proceed with further unwinding, k_u. The processivity calculated using this model is representative of the probability that the helicase will proceed in the unwinding pathway. The model also predicts a slow, rate-limiting step, k_{np}, which describes the conversion of nonproductive UvrD-DNA complexes into active unwinding complexes (39).

described, and ~0.2 nM radiolabeled partial duplex DNA substrate. The reactions were assembled on ice, and the helicase was allowed to preincubate with the DNA substrate for several minutes. The reactions were initiated by the addition of ATP and incubated at 37 °C for 5 min before addition of 8 μl of stop solution, 37.5% (v/v) glycerol, 50 mM EDTA, 0.3% (w/v) SDS, 0.5× TBE and dyes. The reactions were resolved on 12% (w/v) or 8% (w/v) non-denaturing polyacrylamide gels (19:1 cross-linking ratio), or 3% (w/v) NuSieve™ agarose gels depending on substrate size and visualized by PhosphorImaging (GE Healthcare).

Rapid Quench Singe Turnover Assays and Modeling—Rapid quench single turnover assays were performed essentially as previously described (32), with minor modifications, at room temperature (~19 °C) using a computer controlled quenched-flow apparatus (KinTek RQF-3, University Park, PA). Helicase was allowed to incubate with the partial duplex substrate (100 nM helicase, 2 nM DNA substrate) in buffer L (25 mM Tris-HCl (pH 7.5), 200 μg/ml of bovine serum albumin, 200 μM EDTA, 10% (v/v) glycerol, 5 mM 2-mercaptoethanol) plus 3 mM ATP on ice for 15 min and then loaded into the D loop. The opposite E loop was loaded with 6 mM $MgCl_2$ and 3 μM DNA hairpin trap in buffer M (25 mM Tris-HCl (pH 7.5), 25 mM NaCl, 10% (v/v) glycerol, 5 mM 2-mercaptoethanol). Reactions were initiated by rapidly mixing equal volume aliquots of the solutions from loops D and E, and were quenched with 200 mM EDTA and 0.2% (w/v) SDS. Samples were resolved on non-denaturing polyacrylamide gels or 3% (w/v) NuSieve-agarose gels as described above and visualized by PhosphorImaging (GE Healthcare).

The modeled unwinding curves were fit to the data collected with each partial duplex DNA substrate using a linear regression model and the kinetic simulator Tenua (Bililite). Using the previously published step size as a starting reference, the pre-steady state kinetics were modeled using the n-step kinetic scheme (see Scheme 1). The modeled data were compared with the collected data by calculating the residuals for each collected data point at the corresponding point generated by the model. The number of steps, k_{np}, k_d, and k_u, were manually adjusted until a best fit was obtained. The fits that produced the smallest residuals compared with model were defined as best fits. The modeled curves were visually inspected to ensure the quality of the fit. The data for each substrate length was analyzed in this manner and best fits were calculated (see Fig. 5).

DNA Binding Assays—Affinities of the helicases for DNA were determined using electrophoretic mobility shift assays and fluorescence anisotropy as previously described (33–35).

RESULTS

The *uvrD303* allele, containing amino acid substitutions at positions 403 and 404 (D403A, D404A), was originally isolated by Kushner and colleagues (27) in a screen for mutations in regions outside the conserved helicase motifs that impact biological function. Cells expressing this mutant form of UvrD from a plasmid exhibit increased sensitivity to ultraviolet light and methyl methanesulfonate as do cells containing a deletion of the *uvrD* gene. Interestingly, cells expressing *uvrD303* also exhibit an antimutator phenotype (27), whereas a *uvrD*Δ strain has a mutator phenotype (36). A strain containing *uvrD303* in the chromosome exhibits similar phenotypes (28) indicating that the phenotypes observed are not simply due to increased expression of the mutant protein. Importantly, the purified UvrD303 protein was characterized as having a slightly increased specific activity as an ATPase and unwinds partial duplex substrates 10-fold better than the wild-type enzyme (27) leading to its designation as a hyper-helicase. We have used biochemical assays, including pre-steady state, single turnover kinetic experiments, to further understand the mechanistic basis of the increased helicase activity associated with this mutant protein.

The *uvrD303* allele was constructed in an expression plasmid as described under "Materials and Methods" and the protein was purified to apparent homogeneity using a rapid two-step purification procedure (29). To confirm the results presented previously (27), unwinding assays were performed using partial duplex substrates under multiple turnover conditions. All DNA substrates used for these experiments contained a 40-nucleotide poly(dT) 3′-tail and a duplex region of varying length (Table 1). Previous studies have shown that a 40-nucleotide

TABLE 1
Oligonucleotides

Oligonucleotide sequence
RQ24: 5′-GCCCTGCTGCCGACCAACGAAGGT-3′
RQ64: 5′-ACCTTCGTTGGTCGGCAGCAGGGC (T_{40})-3′
RQ90: 5′-GCCCTGCTGCCGACCAACGAAGGTTACATTCCCCGTGCTGGCCGT TTG CGGTTGTCCTGTACCACTCGAAGTAGGAGGGGTGCTCACCGA-3′
RQ130: 5′-TCGGTGAGCACCCCTCCTACTTCGAGTGGTACAGGACAACCGCAA ACGGCCAGCACGGGGAATGTAACCTTCGTTGGTCGGCAGCAGGGC (T_{40})-3′
Hairpin trap: 5′-CCTCGCTGCTTTTTGCAGCGAGGC (T_{30})-3′
Fluorescence anisotropy labeled: 5′-TATCGGCACGTCTCGAGATG-Cy5-3′
Fluorescence anisotropy 40b tail: 5′-CATCTCGAGACGTGCCGATA (T_{40})-3′

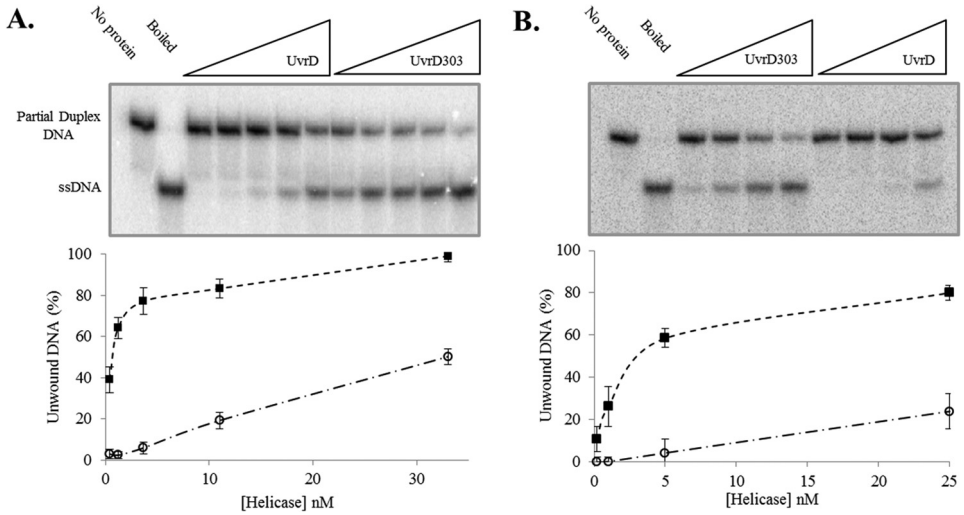

FIGURE 2. **UvrD303 exhibits hyper-helicase activity compared with wild-type UvrD.** *Panel A,* DNA helicase reactions were performed as described under "Materials and Methods" using the 24-bp partial duplex substrate and increasing concentrations of UvrD or UvrD303. The *first two lanes* are controls for no protein and heat-denatured substrate DNA. The *remaining lanes* depict a protein titration of increasing concentration from 0.4 to 33 nM UvrD or UvrD303. Quantitative data from 2 experiments at the indicated concentrations of UvrD (*open circles*) and UvrD303 (*closed squares*) were plotted as the average at each protein concentration. *Error bars* represent the mean ± S.D. *Panel B,* DNA helicase reactions were as described under "Materials and Methods" using the 90-bp partial duplex substrate and increasing concentrations of UvrD or UvrD303. The *first two lanes* are controls for no protein and heat denatured substrate DNA. The *remaining lanes* show a protein titration of increasing concentration from 0.2 to 25 nM UvrD or UvrD303. Quantitative data from 2 experiments at the indicated concentrations of UvrD (*open circles*) and UvrD303 (*closed squares*) were plotted as the average at each protein concentration. *Error bars* represent the mean ± S.D.

ssDNA tail is optimal for UvrD-catalyzed helicase activity (32). Either UvrD or UvrD303 was incubated with the DNA substrate and unwinding was initiated by the addition of ATP. Using a 24-bp partial duplex, the wild-type helicase unwound ~6% of the substrate at a concentration of 3.7 nM as compared with unwinding of 77% of the substrate at an equal concentration of UvrD303 (Fig. 2*A*). This represents nearly a 13-fold increase in unwinding activity. The significant increase in unwinding activity observed with UvrD303 was also demonstrated using a 90-bp partial duplex substrate. On this longer substrate only about 4% of the DNA was unwound by the wild-type helicase at a concentration of 5 nM as compared with 59% unwound by UvrD303 at the same concentration (Fig. 2*B*). These data support previous work showing that UvrD303 exhibits a marked increase in helicase activity under multiple turnover conditions (27).

The multiple turnover unwinding experiments, whereas informative, do not yield significant new information about the mechanism by which the helicase activity is increased. The observed increase could be due to one or more of any number of properties being altered in the mutant including binding affinity for the substrate, an increase in the rate of unwinding, or an increase in the processivity of the unwinding reaction.

The previous study (27) suggested that the increased helicase activity observed in multiple turnover experiments was not due to an increased affinity of UvrD303 for the DNA substrate. To confirm and extend this observation we measured the DNA binding activity of UvrD303, as compared with that of the wild-type UvrD, using both electrophoretic mobility shift assays (EMSA) and fluorescence anisotropy in the presence and absence of nucleotide. EMSA experiments using the 24-bp partial duplex ligand indicated that UvrD and UvrD303 both bound DNA, in the presence and absence of nucleotide, with very similar affinity (Fig. 3, *A* and *C–F*). Fluorescence anisotropy experiments were performed using a fluorescently labeled ligand with 20 bp of duplex DNA and a 40-nucleotide 3′-ssDNA tail to mimic the substrate used in unwinding experiments. Ten individual measurements were made at each protein concentration and the average was plotted as a function of protein concentration (Fig. 3*B*). These experiments yielded a K_d for UvrD of 23.5 ± 1.4 nM in the absence of nucleotide and 14.6 ± 1.4 nM in the presence of the poorly hydrolyzed ATP analog, ATPγS. These values are somewhat higher than previously reported K_d values for UvrD (37), which were determined using a different technique and a different DNA ligand. The K_d measured for UvrD303 was 15.7 ± 2.3 nM in the absence of nucleotide and 3.9 ± 0.6 nM in the presence of ATPγS. These data suggest that UvrD303 has a somewhat higher initial binding affinity for the partial duplex substrate than UvrD. However, this difference in initial DNA binding affinity alone is not likely to

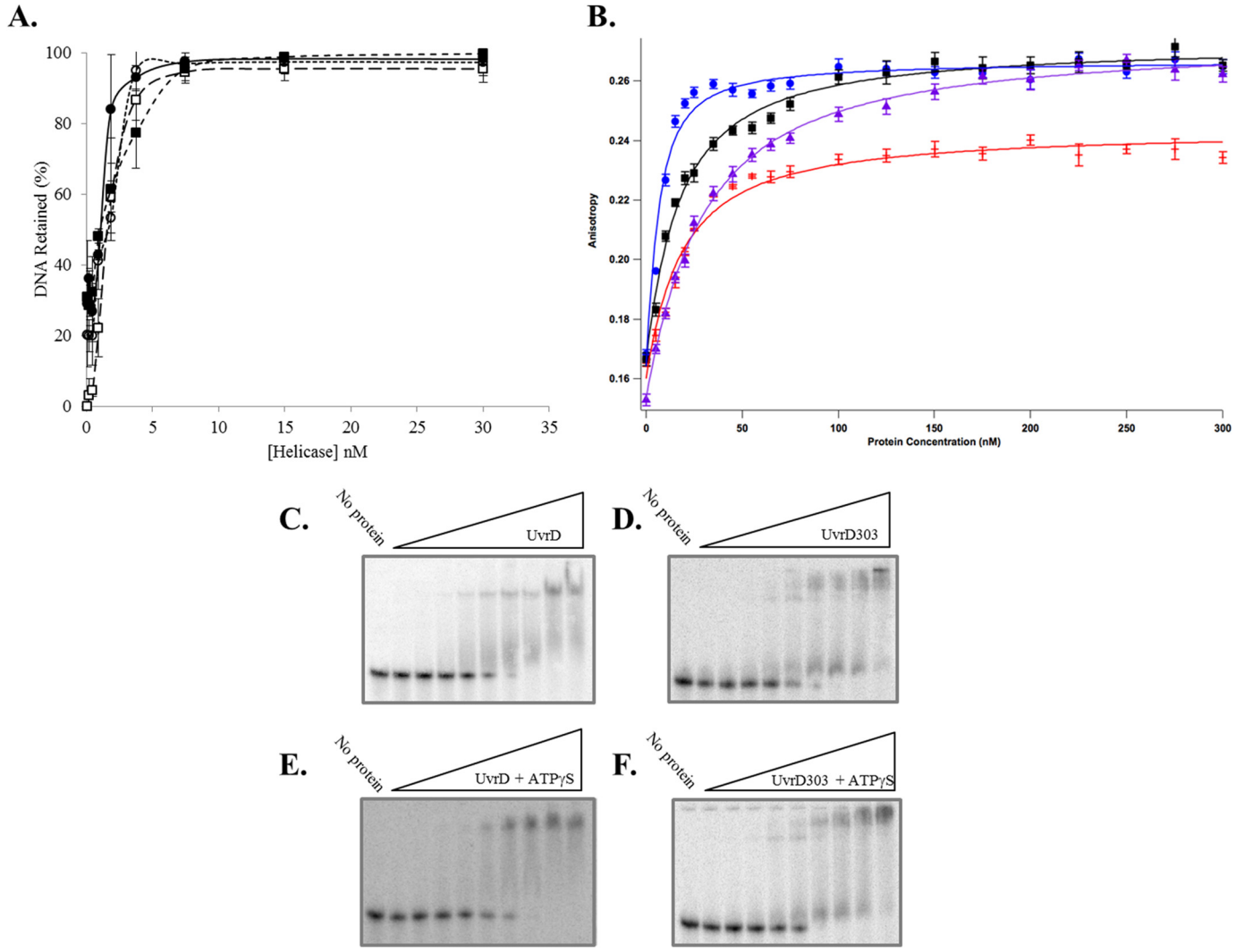

FIGURE 3. **UvrD303 exhibits similar DNA binding properties to that of wild-type UvrD.** *Panel A,* electrophoretic mobility shift assays were performed as described under "Materials and Methods." Increasing concentrations of UvrD (*open circles*), UvrD + ATPγS (*open squares*), UvrD303 (*closed circles*), and UvrD303 + ATPγS (*closed squares*) were incubated with the 24-bp partial duplex substrate for 5 min prior to electrophoresis. Data represent the average of 3 experiments. *Error bars* represent the mean ± S.D. *Panel B,* fluorescence anisotropy was performed as described under "Materials and Methods." Each data point is an average of 10 reads at each indicated protein concentration. The data were collected using a SPEX Fluorolog-3 spectrofluorometer. UvrD303 (*red cross*); UvrD303 + ATPγS (*blue circles*); wild-type UvrD (*purple triangles*); wild-type UvrD + ATPγS (*black squares*). *Panels C-F,* representative EMSA gels with UvrD in the absence of ATP (*panel C*), UvrD303 in the absence of ATP (*panel D*), UvrD in the presence of 3 mM ATPγS (*panel E*), and UvrD303 in the presence of 3 mM ATPγS (*panel F*). *Lane 1*, no protein; *lane 2*, 0.1 nM UvrD/UvrD303; *lane 3*, 0.2 nM UvrD/UvrD303; *lane 4*, 0.5 nM UvrD/UvrD303; *lane 5*, 0.9 nM UvrD/UvrD303; *lane 6*, 1.9 nM UvrD/UvrD303; *lane 7*, 3.8 nM UvrD/UvrD303; *lane 8*, 7.5 nM uvrD/UvrD303; *lane 9*, 15 nM UvrD/UvrD303; *lane 10*, 30 nM UvrD/UvrD303.

account for the dramatic increase in unwinding observed using UvrD303.

To investigate further the increase in UvrD303-catalzyed unwinding, single turnover pre-steady state kinetic experiments were performed. Using a rapid chemical quenched flow protocol, excess helicase (50 nM final concentration), the partial duplex substrate (1 nM final concentration), and ATP were pre-incubated to allow formation of the enzyme-substrate complex, and then rapidly mixed with $MgCl_2$ and a 1500-fold excess of a DNA hairpin trap to initiate unwinding. The excess trap ensures the sequestering of any free or dissociated helicase and prevents any reinitiation of unwinding. Control experiments have demonstrated that the hairpin trap at this concentration is effective in trapping all excess UvrD (data not shown). The time of incubation was varied from 0.075 to 65 s and the fraction of DNA unwound was determined at each time point. Rapid quench flow experiments were performed using the 24- and 90-bp partial duplex substrates described above and a 243-bp partial duplex substrate generated by digestion of pUC19-TS plasmid as described under "Materials and Methods." It is important to note that these unwinding assays are "all or none" and do not detect partially unwound DNA molecules.

Using the 24-bp partial duplex DNA, both UvrD and UvrD303 were capable of converting the duplex substrate to ssDNA (Fig. 4*A*). Under these conditions UvrD unwound ~50% of the substrate, whereas UvrD303 unwound nearly 95% of the substrate. It also appears that the exponential rise trends generated by the unwinding reactions level off at very similar time points. If these trends are compared with respect to the total amount of partial duplex substrate, a simple rate describing the approximate number of base pairs unwound per second per UvrD molecule can be estimated. These rates on this 24-bp

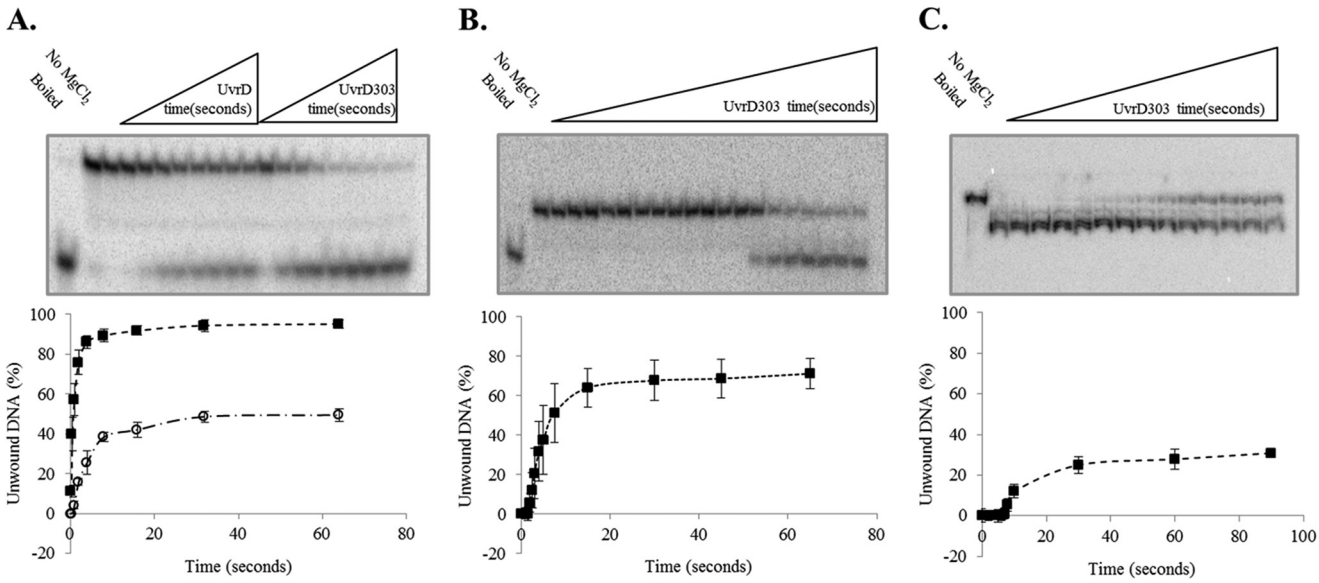

FIGURE 4. **UvrD303 exhibits a stimulated helicase activity in single turnover rapid quench reactions.** *Panel A,* DNA helicase single turnover rapid quench reactions were performed as described under "Materials and Methods" using a 24-bp partial duplex substrate and increasing time. The *first two lanes* are controls for heat denatured substrate and for no magnesium chloride ($MgCl_2$). The *remaining lanes* depict a time course from 0.25 to 64 s for both UvrD and UvrD303. Quantitative data from 3 experiments for UvrD (*open circles*) and UvrD303 (*filled squares*) were plotted as an average. *Error bars* represent the mean ± S.D. *Panel B,* DNA helicase single turnover rapid quench reactions were performed as described under "Materials and Methods" using a 90-bp partial duplex substrate and increasing time. The *first two lanes* are controls for heat-denatured substrate and no magnesium chloride ($MgCl_2$). The *remaining lanes* depict a time course from 0.075 to 65 s for UvrD303. Quantitative data represent the average of 3 experiments using UvrD303. *Error bars* represent mean ± S.D. *Panel C,* DNA helicase single turnover rapid quench reactions were performed as described under "Materials and Methods" using a 243-bp partial duplex substrate and increasing time. The *first two lanes* are controls for heat-denatured substrate and no magnesium chloride ($MgCl_2$). The *remaining lanes* depict a time course from 2 to 90 s for UvrD303. Quantitative results from 4 experiments were averaged and plotted for UvrD303. *Error bars* represent the mean ± S.D.

TABLE 2

DNA-stimulated ATPase activity of UvrD and UvrD303

All ATPase assays were performed as described under "Materials and Methods" and measured the production of [^{32}P]ADP as a function of time and helicase (monomer) concentration.

Enzyme	ATPase activity	K_m
	pmol ADP/UvrD/s	*μM*
UvrD	28.5 ± 8.1	64.3 ± 2.7
UvrD303	68.9 ± 27.2	71.1 ± 1.4

partial duplex substrate are estimated to be 0.13 bp unwound per second per UvrD and 0.19 bp unwound per second per UvrD303. These data suggest that the unwinding reaction catalyzed by UvrD and UvrD303 occurs at a similar rate but UvrD303 is able to unwind a much larger fraction of the substrate.

The similarity of the rates of unwinding prompted us to also measure the rate of ATP hydrolysis by the wild-type and mutant protein. Previous data (27) suggested there was a modest increase in ATP hydrolysis activity conveyed by the 303 mutation. However, the K_m for ATP was nearly identical for each helicase. We performed similar ATPase assays and observed the same result. UvrD303 does have a somewhat higher ATPase activity and the K_m of the protein for ATP is essentially identical to that of the wild-type enzyme (Table 2).

When rapid quench flow experiments were performed using the 90-bp partial duplex no detectable unwinding by UvrD was observed. This result was expected as previous work indicates the processivity of UvrD is 40–50 base pairs unwound per binding event (39). Therefore, UvrD is not expected to unwind a 90-bp partial duplex substrate in a single turnover experiment. UvrD303, however, was able to unwind nearly 70% of the 90-bp substrate (Fig. 4*B*).

Because UvrD303 unwound a significant fraction of the 90-bp partial duplex substrate in a single turnover we designed a longer 243-bp partial duplex molecule to begin to test the processivity limits of the mutant helicase. Wild-type UvrD was not tested on this longer substrate because it failed to unwind the 90-bp substrate under single turnover conditions. Significant unwinding activity under single turnover conditions was also observed using the 243-bp partial duplex where UvrD303 was able to unwind ~30% of the substrate (Fig. 4*C*). Taken together, these data suggest that UvrD and UvrD303 unwind duplex DNA with similar rates but the processivity of the unwinding reaction catalyzed by UvrD303 is significantly higher than that of wild-type UvrD.

The augmented helicase activity observed in the single turnover experiments reported above could indicate a change in the kinetic mechanism of unwinding by the helicase. Alternatively, these data may indicate that the kinetic mechanism is essentially the same as that of wild-type UvrD but the processivity of the unwinding reaction has been significantly increased due to the mutation in the 2B subdomain. The unwinding kinetics of UvrD were previously modeled by Ali and Lohman (39) and conform to the well documented *n*-step model of unwinding applied to many DNA helicases (39, 40). In this model, wild-type UvrD has been shown to have a kinetic step size of approximately 4 bp and takes about 10 steps before dissociating from the DNA. Thus, the average processivity of UvrD is 40–50 bp unwound per binding event.

The *n*-step model is shown in Scheme 1. UvrD bound to the partial duplex DNA undergoes a poorly understood conversion from a non-productive complex to an active unwinding complex (k_{np}). It should be noted that k_{np} represents not only the

A.

	UvrD	UvrD303		
Duplex Size	24bp	24bp	90bp	243bp
Amplitude	0.48	0.93	0.71	0.28
Processivity	0.88	0.98	0.97	0.97
Step Size	5 bp	8 bp	7 bp	6 bp
k_{np}	$1.09s^{-1}$	$1.85s^{-1}$	$0.23s^{-1}$	$0.05s^{-1}$
k_u	$6.70s^{-1}$	$5.80s^{-1}$	$5.55s^{-1}$	$6.30s^{-1}$
k_d	$0.41s^{-1}$	$0.65s^{-1}$	$0.58s^{-1}$	$0.54s^{-1}$

B.

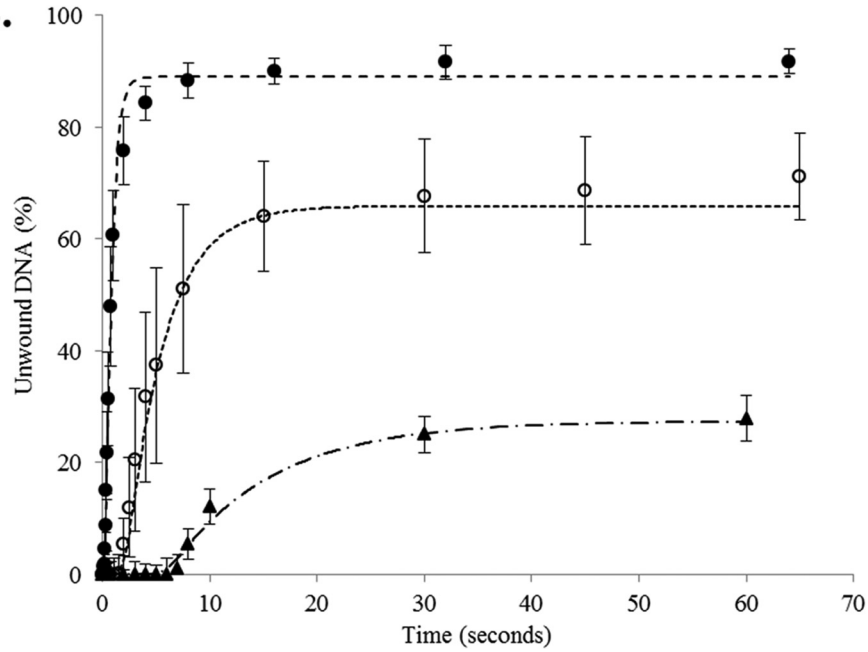

FIGURE 5. **Modeled kinetics of UvrD303 helicase activity.** *Panel A,* compiled data for kinetic parameters of the *n*-step model for UvrD303 on the 24-bp partial duplex, 90-bp partial duplex, or 243-bp partial duplex. *Panel B*, graphical fit of modeled data *versus* collected data. The *hashed lines* represent the unwinding predicted by the model, whereas the markers depict the average data collected from single turnover rapid quench experiments for the 24-bp partial duplex (*closed circles*), the 90-bp partial duplex (*open circles*), and the 243-bp partial duplex (*closed triangles*). *Error bars* represent the mean ± S.D.

conversion to a productive unwinding complex, but the lag from the initiation of unwinding to the point at which completely unwound ssDNA is detectable. Using these parameters, k_{np} "slows" with increasing substrate length (Fig. 5*A*). Once unwinding is initiated, the unwinding scheme assumes that UvrD has a chance to dissociate at each intermediate step (k_d) and a chance to continue unwinding (k_u). The mechanism continues with the helicase taking a size-defined "kinetic step" between each intermediate until either the duplex is unwound or the helicase dissociates from the substrate. The probability of the helicase taking another unwinding step as opposed to dissociating from the substrate is defined as the processivity. Wild-type UvrD was previously modeled to have an average step size of 4.4 bp and a processivity of 0.9. We applied this model to our data using the kinetic simulator Tenua (Bililite). The resulting best fits for the data (Fig. 5*B*) were used to calculate the processivity of the helicases. Using the data reported here for wild-type UvrD unwinding of the 24-bp partial duplex we observed a step size of 4.0 and a processivity of 0.87. These values are in excellent agreement with those reported previously (39) and suggest that UvrD can unwind ~35 bp in a single turnover.

TABLE 3

The 303 mutation confers an increased processivity and step size compared to wild-type

The modeled data were used in conjunction with the following equations: $A_L = P^{(L/m)}$ and $p = (N\text{-}1)/N$ to calculate step size, processivity, and number of bases unwound where A_L is the extent of unwinding, P is processivity, L is duplex length, m is the average step size, and N is the average number of steps taken in a single turnover (39).

	UvrD	UvrD303
Processivity	0.87 ± 0.008	0.973 ± 0.003
Step size	4 bases	7 bases
Steps taken	8.9 ± 0.97	37.4 ± 4.8
Bases unwound	34.9 ± 3.9	261 ± 33.5

When the model is applied to the single turnover data obtained using UvrD303 for the three partial duplex substrates studied here, two striking differences are observed. The average kinetic step size and processivity of UvrD303 increase to an average of 7.0 and 0.973, respectively, as shown in Table 3. This

correlates to an average of 37 steps taken or 261 bp unwound before dissociation. The observed increase in the number of base pairs unwound per binding event is an approximate 8-fold increase and accounts for the previously reported 10-fold increase in helicase activity.

DISCUSSION

The *uvrD303* allele was discovered in a screen for mutations outside the conserved helicase motifs of UvrD that had a clear impact on the activity of the protein as measured in genetic assays (27). UvrD303 contains two amino acid substitutions (D403A, D404A) in the 2B subdomain of the protein between conserved motifs IV and V (see Fig. 1*B*). The impact of this mutation is remarkable both for its alteration of the biochemistry of the protein and the significantly different phenotype of cells harboring this mutation. The purified protein has been described as a hyper-helicase based on a steady state analysis of helicase activity. This has been confirmed in our studies (see Fig. 2). Expression from a plasmid or the chromosome confers an antimutator phenotype on cells suggesting an altered, but still functional, role in MMR. Curiously, cells harboring the *uvrD303* mutation are UV-sensitive as are *uvrD* null mutants. Sandler and colleagues (28) have traced this phenotype to a defect in recombinational repair of UV-induced lesions rather than a defect in NER and conclude that UvrD303 is likely functional in NER. This is consistent with the fact that UvrD303 is active as a helicase and with the hypo-recombination phenotype associated with the *uvrD303* allele (27). *uvrD* null mutants exhibit a hyper-recombination phenotype that has been ascribed to the ability of wild-type UvrD to strip RecA protein from potential recombination intermediates (38). Thus, wild-type UvrD prevents unwanted recombination events from occurring and, in the absence of UvrD, there is more recombination than in wild-type cells. The hypo-recombination phenotype associated with *uvrD303* may be due to an increased ability to disrupt RecA-DNA filaments poised to undergo recombination. The experiments reported here have shed light on the altered properties of UvrD303 and provide some insight into why cells harboring UvrD303 exhibit antimutator and hypo-Rec phenotypes.

The pre-steady state, single turnover experiments shown in Fig. 4 indicate that UvrD303 has an increased processivity and an increased kinetic step size. In fact, the processivity of the mutant protein is increased by a factor of 8 from ~40 bp per unwinding event to nearly 300 bp unwound per unwinding event. This result is sufficient to explain the increased helicase activity observed in steady state experiments (27) (Fig. 2) and, coupled with the fact that the rate of unwinding catalyzed by UvrD303 is essentially the same as for the wild-type protein, suggests that the primary biochemical alteration in the enzyme is an increase in processivity. However, we also note there is an increase in the affinity of UvrD303, as compared with wild-type UvrD, for initial binding to a DNA substrate as measured using fluorescence anisotropy. Because the single turnover experiments demonstrating an increase in the processivity of the unwinding reaction are done under conditions of excess enzyme this is not likely to be a significant factor in determining the processivity of unwinding. Nonetheless, this may contribute to the observed hyper-helicase activity measured in multiple turnover experiments and could have an impact *in vivo*.

How might the 2-amino acid mutation within the 2B subdomain of UvrD increase the processivity of the enzyme? It has been shown that the 2B subdomain of SF1 helicases has a role in regulating the helicase activity of the enzyme (41). Deletion of the 2B subdomain in the very closely related Rep helicase has been shown to activate the helicase activity of a Rep monomer (26) consistent with the 2B subdomain having a role in regulating helicase activity. Efforts to delete the 2B subdomain of UvrD have not been successful and it has been suggested that perhaps the unregulated activity of UvrD is lethal (25).

A possible explanation for the increase in processivity is that UvrD303 forms dimers more efficiently than the wild-type protein. The impact of more efficient dimer formation is not likely to be reflected in single turnover experiments done with an excess of enzyme because the substrate is prebound with protein prior to initiating the unwinding reaction. Alternatively, the dimers might be more stable during the course of the unwinding reaction serving to increase the processivity. We cannot formally discount this possibility.

The explanation for the increased processivity that we propose takes into account the mechanistic insights derived from various co-crystal structures and the proposal that the 2B domain plays a regulatory role. The crystal structure of UvrD with the 2B subdomain in the open conformation has been reported (22). This open conformation of UvrD differs from its closed counterpart by a 160° rotation of the 2B subdomain around the 2A subdomain. The closed conformation, as captured by Lee and Yang (14), showed that the 2B subdomain makes contacts with the duplex DNA and the newly unwound ssDNA as well as having contacts with the 1B subdomain. The two conformations of UvrD (open and closed) differ only slightly from the two conformations of Rep protein reported earlier (20). Recently it has been shown that the 2B subdomain of UvrD exists in many intermediate positions between completely open and completely closed depending on factors such as salt concentration, DNA, and nucleotide binding (22). We speculate that the UvrD303 mutation prevents the helicase from adopting a fully closed conformation with respect to the 2B subdomain perhaps because the mutant 2B subdomain is unable to make or maintain contacts with the 1B subdomain. Although our current attempts at localizing the "contact points" of the 2B and 1B subdomains have not been successful (data not shown), it may be possible to construct a helicase that exhibits UvrD303-like hyper-helicase activity via mutations in the 1B subdomain.

Lee and Yang (14) have proposed an alternative mode of unwinding based on the translocation of the protein along one strand with the helicase acting to "plow through" and displace the partner strand as contrasted with the wrench-and-inchworm model for unwinding proposed based on structural studies of UvrD bound to varying DNA substrates and nucleotides. In the latter model, the 2B subdomain engages the duplex DNA via the so called GIG motif and, along with the ssDNA anchor of motif III, holds the DNA substrate, whereas the separation pin and ssDNA gateway remain flexible allowing for unwinding. As the helicase cycles through the process of ATP hydrolysis these four contact points invert their roles allowing the helicase to act

as a sort of "molecular ratchet" in the course of the unwinding reaction. We speculate that UvrD303 utilizes the strand displacement mode of unwinding exclusively due to the mutations in the 2B subdomain. This interpretation is consistent with the increased processivity we have measured with the mutant protein and, remarkably, the increased processivity reported here mirrors the processivity reported for UvrD as a translocase (42). In addition, an alternate mode of unwinding may account for the near doubling in kinetic step size observed for UvrD303. It is reasonable to expect a different unwinding mechanism to exhibit a different kinetic step size.

It is possible that opening and closing of the 2B subdomain modulates the unwinding activity of UvrD and this, in turn, directs its function in some of its intracellular roles. It was reported that UvrD303 removes RecA from sites of DNA damage to a greater extent than wild-type UvrD when expressed from the chromosome (28). These data would suggest that the 303 mutation alters the function of UvrD in its role in RecA-mediated DNA repair. Wild-type UvrD has been shown to remove RecA from RecA-ssDNA filaments (38) and presumably this is regulated such that UvrD destroys unwanted recombination intermediates, while not interfering with those intermediates that are required for appropriate recombinational repair. How this activity of UvrD is regulated is unknown. It is tempting to speculate that UvrD303 is hyperactive in this function and this leads to the hypo-Rec phenotype associated with the mutant. Indeed, if UvrD303 simply translocates along ssDNA acting as a helicase by plowing through the duplex then this mechanism might also remove bound protein, like RecA.

In addition, it has been shown that when UvrD303 is expressed from the chromosome there is a *decrease* in the rate of spontaneous mutation by 50–80% (27, 28). UvrD has a well described role in MMR as the helicase that unwinds the duplex DNA between the nick that initiates this repair reaction and the mismatched base pair that must be repaired. As the DNA is unwound the nascent ssDNA is removed by ssDNA exonucleases providing a gap that is filled by DNA polymerase III to complete the repair reaction. The nick that initiates MMR is located on the unmethylated strand at a hemi-methylated d(GATC) site. This site may be located at a significant distance from the mismatched base pair that must be replaced to complete repair. The efficiency of this repair reaction decreases as the distance between the hemi-methylated d(GATC) and the mismatch increases (43), perhaps due to the limited processivity of UvrD. A UvrD mutant with an increased processivity could be envisioned to improve the efficiency of mismatch repair over long distances and this may account for the antimutator phenotype associated with the *uvrD303* mutation. This hypothesis has not been directly tested.

Acknowledgments—We thank Susan Whitfield for help in preparing the artwork and members of the Matson laboratory for careful reading of the manuscript.

REFERENCES

1. Matson, S. W., Bean, D. W., and George, J. W. (1994) DNA helicases: enzymes with essential roles in all aspects of DNA metabolism. *Bioessays* **16,** 13–22
2. Egelman, E. H. (1998) Bacterial helicases. *J. Struct. Biol.* **124,** 123–128
3. Bochman, M. L., and Schwacha A. (2009) The Mcm complex: unwinding the mechanism of a replicative helicase. *Microbiol. Mol. Biol. Rev.* **73,** 652–683
4. Abdelhaleem, M. (2010) Helicases: an overview. *Methods Mol. Biol.* **587,** 1–12
5. Bachrati, C. Z., and Hickson, I. D. (2008) RecQ helicases: guardian angels of the DNA replication fork. *Chromosoma* **117,** 219–233
6. Chu, W. K., and Hickson, I. D. (2009) RecQ helicases: multifunction genomic caretakers. *Nat. Rev. Cancer* **9,** 644–654
7. Gupta, R., and Brosh R. M., Jr. (2007) DNA repair helicases as targets for anti-cancer therapy. *Curr. Med. Chem.* **14,** 503–517
8. Brosh, R. M., Jr., and Bohr, V. A. (2007) Human premature aging, DNA repair and RecQ helicases. *Nucleic Acids Res.* **35,** 7527–7544
9. Husain, I., Van Houten, B., Thomas, D. C., Abdel-Monem, M., and Sancar, A. (1985) Effect of DNA polymerase I and DNA helicase II on the turnover rate of UvrABC excision nuclease. *Proc. Natl. Acad. Sci. U.S.A.* **82,** 6774–6778
10. Yamaguchi, M., Dao, V., and Modrich, P. (1998) MutS and MutL activate DNA helicase II in a mismatch dependent manner. *J. Biol. Chem.* **273,** 9197–9201
11. Lahue, R. S., Au, K. G., and Modrich, P. (1989) DNA mismatch correction in a defined system. *Science* **245,** 160–164
12. Dao, V., and Modrich, P. (1998) Mismatch-, MutS-, MutL-, and helicase II- dependent unwinding from the single-strand break of an incised heteroduplex. *J. Biol. Chem.* **273,** 9202–9207
13. Centore, R. C., and Sandler, S. J. (2007) UvrD limits the number and intensities of RecA-green fluorescent protein structures in *Escherichia coli* K-12. *J. Bacteriol.* **189,** 2915–2920
14. Lee, J. Y., and Yang, W. (2006) UvrD helicase unwinds DNA one base pair at a time by a two-part power stroke. *Cell* **127,** 1349–1360
15. Gorbalenya, A. E., and Koonin, E. V. (1993) Helicases: amino acid sequence comparisons and structure-function relationships. *Curr. Opin. Struct. Biol.* **3,** 419–429
16. Iyer, L. M., Leipe, D. D., Koonin, E. V., and Aravind, L. (2004) Evolutionary history and higher order classification of AAA^+ ATPases. *J. Struct. Biol.* **146,** 11–31
17. Hickson, I. D., Arthur, H. M., Bramhill, D., and Emmerson, P. T. (1983) The *E. coli* uvrD gene product is DNA helicase II. *Mol. Gen. Genet.* **190,** 265–270
18. Matson, S. W., and George, J. W. (1987) DNA helicase II of *Escherichia coli*: characterization of the single-stranded DNA-dependent NTPase and helicase activities. *J. Biol. Chem.* **262,** 2066–2076
19. Velankar, S. S., Soultanas, P., Dillingham, M. S., Subramanya, H. S., and Wigley, D. B. (1999). Crystal structures of complexes of PcrA DNA helicase with a DNA substrate indicate an inchworm mechanism. *Cell* **97,** 75–84
20. Korolev, S., Hsieh, J., Gauss, G. H., Lohman, T. M., and Waksman, G. (1997) Major domain swiveling revealed by the crystal structures of complexes of *E. coli* Rep helicase bound to single-stranded DNA and ADP. *Cell* **90,** 635–647
21. Matson, S. W. (1986) Escherichia coli helicase II (uvrD gene product) translocates unidirectionally in a 3′ to 5′ direction. *J. Biol. Chem.* **261,** 10169–10175
22. Jia, H., Korolev, S., Niedziela-Majka A., Maluf, N. K., Gauss, G. H., Myong, S., Ha, T., Waksman, G., and Lohman, T. M. (2011) Rotations of the 2B sub-domain of *E. coli* UvrD helicase/translocase coupled to nucleotide and DNA binding. *J. Mol. Biol.* **411,** 633–9648
23. Yao, N., Reichert, P., Taremi, S. S., Prosise, W. W., and Weber, P. C. (1999) Molecular views of viral polyptrotein processing revealed by the crystal structure of the hepatitis C virus bifunctional protease-helicase. *Structure* **7,** 1353–1363
24. Appleby, T. C., Anderson, R., Fedorova, O., Pyle, A. M., Wang, R., Liu, X., Brendza, K. M., and Somoza, J. R. (2011) Visualizing ATP-dependent RNA translocation by the NS3 helicase from HCV. *J. Mol. Biol.* **405,** 1139–1153
25. Cheng, W., Brendza, K. M., Gauss, G. H., Korolev, S., Waksman, G., and Lohman, T. M. (2002) The 2B domain of the *Escherichia coli* Rep protein is not required for DNA helicase activity. *Proc. Natl. Acad. Sci. U.S.A.* **99,**

16006–16011
26. Brendza, K. M., Cheng, W., Fischer, C. J., Chesnik, M. A., Niedziela-Majka, A., and Lohman, T. M. (2005) Autoinhibition of *Escherichia coli* Rep monomer helicase activity by its 2B subdomain. *Proc. Natl. Acad. Sci. U.S.A.* **102,** 10076–10081
27. Zhang, G., Deng, E., Baugh, L., and Kushner, S. R. (1998) Identification and characterization of *Escherichia coli* DNA helicase II mutants that exhibit increased unwinding efficiency. *J. Bacteriol.* **180,** 377–387
28. Centore, R. C., Leeson, M. C., and Sandler, S. J. (2009) UvrD303, a hyper-helicase mutant that antagonizes RecA-dependent SOS expression by a mechanism that depends on its C terminus. *J. Bacteriol.* **191,** 1429–1438
29. Tahmaseb K., and Matson, S. W. (2010) Rapid purification of helicase proteins and *in vitro* analysis of helicase activity. *Methods* **51,** 322–328
30. Studier F. W. (2005) Protein production by autoinduction in high-density shaking cultures. *Protein Expr. Purif.* **41,** 207–234
31. Runyon, G. T., Wong, I., and Lohman, T. M. (1993) Overexpression, purification, DNA binding and dimerization of the *Esherichia coli* uvrD gene product (helicase II). *Biochemistry* **32,** 602–612
32. Ali, J. A., Maluf, N. K., and Lohman, T. M. (1999) An oligomeric form of *E. coli* UvrD is required for optimal helicase activity. *J. Mol. Biol.* **293,** 815–834
33. Mechanic, L. E., Frankel, B. A., and Matson, S. W. (2000) *Escherichia coli* MutL loads DNA helicase II onto DNA. *J. Biol. Chem.* **275,** 38337–38346
34. Yang, Y., Sass, L. E., Du, C., Hsieh, P., and Erie, D. A. (2005) Determination of protein-DNA binding constants and specificities from statistical analyses of single molecules: MutS-DNA interactions. *Nucleic Acids Res.* **33,** 4322–4334
35. Geng, H., Sakato, M., DeRocco, V., Yamane, K., Du, C., Erie, D. A., Hingorani, M., and Hsieh, P. (2012) Biochemical analysis of the human mismatch repair proteins hMutSa MSH2(G674A)-MSH6 and MSH2-MSH6(T1219D). *J. Biol. Chem.* **287,** 9777–9791
36. Washburn, B. K., and Kushner, S. R. (1991) Construction and analysis of deletions in the structural gene (*uvrD*) for DNA helicase II of *Escherichia coli*. *J. Bacteriol.* **173,** 2569–2575
37. Hall, M. C., Ozsoy, A. Z., and Matson, S. W. (1998) Site-directed mutations in motif VI of *Escherichia coli* DNA helicase II result in multiple biochemical defects: evidence for the involvement of motif VI in the coupling of ATPase and DNA binding activities via conformational changes. *J. Mol. Biol.* **277,** 257–271
38. Veaute, X., Delmas, S., Selva, M., Jeusset, J., Le Cam, E., Matic, I., Fabre, F., and Petit, M. A. (2005) UvrD helicase, unlike Rep helicase, dismantles RecA nucleoprotein filaments in *Escherichia coli*. *EMBO J.* **24,** 180–189
39. Ali, J. A., and Lohman, T. M. (1997) Kinetic measurement of the step size of DNA unwinding by *Escherichia coli* UvrD helicase. *Science* **275,** 377–380
40. Maluf, N. K., Ali, J. A., and Lohman, T. M. (2003) Kinetic mechanism for formation of the active, dimeric UvrD helicase-DNA complex. *J. Biol. Chem.* **278,** 31930–31940
41. Lohman, T. M., Tomko, E. J., and Wu, C. G. (2008) Non-hexameric DNA helicases and translocases: mechanisms and regulation. *Nat. Rev. Mol. Cell Biol.* **9,** 391–401
42. Tomko, E. J., Fischer, C. J., and Lohman, T. M. (2012) Single-stranded DNA translocation of E. coli UvrD monomer is tightly coupled to ATP hydrolysis. *J. Mol. Biol.* **418,** 32–46
43. Bruni, R., Martin, D., and Jiricny, J. (1988) d(GATC) sequences influence *Escherichia coli* mismatch repair in a distance-dependent manner from positions both upstream and downstream of the mismatch. *Nucleic Acids Res.* **16,** 4875–4890